Hindawi Publishing Corporation
Journal of Biomedicine and Biotechnology
Volume 2012, Article ID 368075, 8 pages
doi:10.1155/2012/368075

Research Article

^{111}In-Labeled Cystine-Knot Peptides Based on the Agouti-Related Protein for Targeting Tumor Angiogenesis

Lei Jiang,[1,2] Zheng Miao,[2] Richard H. Kimura,[2] Adam P. Silverman,[3] Gang Ren,[2] Hongguang Liu,[2] Hankui Lu,[1] Jennifer R. Cochran,[3] and Zhen Cheng[2]

[1] *Department of Nuclear Medicine, Shanghai Sixth People's Hospital, Shanghai Jiao Tong University, Shanghai 200233, China*
[2] *Molecular Imaging Program at Stanford (MIPS), Department of Radiology, Stanford Cancer Institute, and Bio-X Program, Canary Center at Stanford for Cancer Early Detection, Stanford University, Stanford, CA 94305, USA*
[3] *Department of Bioengineering, Stanford Cancer Institute, and Bio-X Program, Stanford University, Stanford, CA 94305, USA*

Correspondence should be addressed to Zhen Cheng, zcheng@stanford.edu

Received 14 December 2011; Revised 29 January 2012; Accepted 30 January 2012

Academic Editor: David J. Yang

Agouti-related protein (AgRP) is a 4-kDa cystine-knot peptide of human origin with four disulfide bonds and four solvent-exposed loops. The cell adhesion receptor integrin $\alpha_v\beta_3$ is an important tumor angiogenesis factor that determines the invasiveness and metastatic ability of many malignant tumors. AgRP mutants have been engineered to bind to integrin $\alpha_v\beta_3$ with high affinity and specificity using directed evolution. Here, AgRP mutants 7C and 6E were radiolabeled with ^{111}In and evaluated for *in vivo* targeting of tumor integrin $\alpha_v\beta_3$ receptors. AgRP peptides were conjugated to the metal chelator 1, 4, 7, 10-tetra-azacyclododecane-N, N′, N″, N‴-tetraacetic acid (DOTA) and radiolabeled with ^{111}In. The stability of the radiopeptides ^{111}In-DOTA-AgRP-7C and ^{111}In-DOTA-AgRP-6E was tested in phosphate-buffered saline (PBS) and mouse serum, respectively. Cell uptake assays of the radiolabeled peptides were performed in U87MG cell lines. Biodistribution studies were performed to evaluate the *in vivo* performance of the two resulting probes using mice bearing integrin-expressing U87MG xenograft tumors. Both AgRP peptides were easily labeled with ^{111}In in high yield and radiochemical purity (>99%). The two probes exhibited high stability in phosphate-buffered saline and mouse serum. Compared with ^{111}In-DOTA-AgRP-6E, ^{111}In-DOTA-AgRP-7C showed increased U87MG tumor uptake and longer tumor retention (5.74 ± 1.60 and 1.29 ± 0.02%ID/g at 0.5 and 24 h, resp.), which was consistent with measurements of cell uptake. Moreover, the tumor uptake of ^{111}In-DOTA-AgRP-7C was specifically inhibited by coinjection with an excess of the integrin-binding peptidomimetic c(RGDyK). Thus, ^{111}In-DOTA-AgRP-7C is a promising probe for targeting integrin $\alpha_v\beta_3$ positive tumors in living subjects.

1. Introduction

Molecular imaging is a rapidly evolving field in biomedical research and provides powerful techniques to noninvasively study a variety of important characteristics of cancers, such as tumor metabolism, proliferation, hypoxia, and receptor expression [1–3]. Therefore, novel molecular probes that target these characteristics have been under active and intensive development and investigation. Many platforms including small molecules, peptides, proteins, and nanoparticles have been explored in order to develop molecular probes to image a variety of important disease biomarkers [4, 5].

Cystine-knot peptides consist of a stable core motif of at least three disulfide bonds that are interwoven into a "knot" conformation. There is great sequence diversity among cystine-knot family members, as only the disulfide-bonded core is conserved; consequently, the loops connecting the cysteine residues are highly tolerant to substitution or incorporation of additional amino acid residues [6–8]. Previously, we used a truncated form of the Agouti-related protein (AgRP*), a 4-kDa cystine-knot peptide with four disulfide bonds and four solvent-exposed loops, as a molecular scaffold for directed evolution. In this study, high-throughput methods were used to screen a yeast-displayed

Table 1: Amino acid sequences of the AgRP* mutants 7C and 6E used in this study. DOTA was site-specific conjugated to the N-terminal amine of these peptides.

AgRP*	GCVRLHESCLGQQVPCCDPAATCYCRFFNAFCYCR
AgRP-6E	GCVRLHESCLGQQVPCCDPAATCYCVERGDGNRRCYCR
AgRP-7C	GCVRLHESCLGQQVPCCDPAATCYCYGRGDNDLRCYCR

Red lines represent the disulfide bonds between Cys^1–Cys^4, Cys^2–Cys^5, Cys^3–Cys^8, and Cys^6–Cys^7 in the AgRP*-based cystine-knot peptides.

AgRP* library to identify several mutants with high affinity and specificity for $\alpha_v\beta_3$ integrin [8].

The cell adhesion receptor integrin $\alpha_v\beta_3$ is an important tumor angiogenesis factor that determines the invasiveness and metastatic ability of many malignant tumors. It is upregulated on the tumor cell surface and also overexpressed on activated endothelial cells around the tumor tissues [9–11]. Many radiolabeled probes have been developed for imaging integrin expression using positron emission tomography (PET) or single-photon emission computed tomography (SPECT) [12–15]. In our recent research, the ^{64}Cu-DOTA conjugated AgRP* mutant 7C (^{64}Cu-DOTA-AgRP-7C) was successfully developed for PET imaging of integrin $\alpha_v\beta_3$ positive tumors. This study demonstrated the potential of AgRP*-based integrin-binding peptides for use as *in vivo* molecular imaging applications and highlighted cystine-knots as promising molecules for further development as diagnostics or therapeutics against different tumor targets [13].

In the current study, to further characterize the *in vivo* performance of integrin-binding AgRP*-based peptides and also evaluate their potential use for SPECT imaging applications, two DOTA-conjugated AgRP* mutants (DOTA-AgRP-7C and DOTA-AgRP-6E; Table 1) were synthesized and radiolabeled with the gamma emitter ^{111}In ($t_{1/2}$ = 2.8 days). Tumor uptake, biodistribution, and stability of the resulting probes were evaluated in integrin $\alpha_v\beta_3$ positive human glioblastoma U87MG tumor xenograft models.

2. Materials and Methods

2.1. Chemicals, Reagents, and Instruments. DOTA-AgRP-7C and DOTA-AgRP-6E were synthesized and reported previously [13]. $^{111}InCl_3$ was purchased from PerkinElmer. All other reagents were obtained from Fisher Scientific Co. unless otherwise specified. Female athymic nude mice (nu/nu, 5-6 weeks old) were purchased from Charles River Laboratory (Wilmington, MA, USA). A CRC-15R PET dose calibrator (Capintec Inc., Ramsey, NJ, USA) was used for all radioactivity measurements. Reversed phase high performance liquid chromatography (RP-HPLC) was performed on a Dionex Summit HPLC system (Dionex Corporation, Sunnyvale, CA, USA) equipped with a 170 U 4-Channel UV-Vis absorbance detector and radioactivity detector (Carroll and Ramsey Associates, model 105S, Berkeley, CA). UV detection wavelengths were 218 nm, 254 nm, and 280 nm for all the experiments. Both semipreparative (Vydac, Hesperia, CA. 218TP510-C18, 10 mm × 250 mm) and analytical RP-HPLC columns were used. The mobile phase was solvent A, 0.1% trifluoroacetic acid (TFA)/H_2O, and solvent B, 0.1%TFA/acetonitrile.

2.2. Cell Line and Cell Culture. The human glioblastoma cell line U87MG was obtained from American Type Culture Collection (ATCC; Manassas, VA, USA). The cells were maintained as monolayer cultures in Dulbecco's Modified Eagle Medium (DMEM) containing high glucose (GIBCO, Carlsbad, CA, USA), which was supplemented with 10% fetal bovine serum (FBS; GIBCO) and 1% penicillin-streptomycin (GIBCO). The cells were expanded in tissue culture dishes and kept in a humidified atmosphere of 5% CO_2 at 37°C. The media was changed every other day. A confluent monolayer was detached with 0.5% Trypsin-EDTA, 0.01 M PBS (pH 7.4), and dissociated into a single-cell suspension for further cell culture and binding experiments.

2.3. Peptide Radiolabeling. DOTA-AgRP-7C or DOTA-AgRP-6E were radiolabeled with ^{111}In by incubating 15 μg of peptide in 37 MBq (1 mCi) $^{111}InCl_3$ and 100 μL of 0.1 N NH_4OAc (pH 5.0–5.5) buffer, at 80°C for 45 min. The radiolabeled conjugates, ^{111}In-DOTA-AgRP-7C or ^{111}In-DOTA-AgRP-6E, were purified using a PD-10 column (GE Healthcare Life Sciences, Piscataway, NJ, USA) and eluted with PBS.

2.4. In Vitro Stability Assays. Radiolabeled AgRP* peptides were incubated in 0.01 M PBS (pH 7.4) at 37°C for 24 h and monitored for degradation by HPLC. Stability was also tested by incubating 0.74 MBq (20 μCi) ^{111}In-DOTA-AgRP-7C or ^{111}In-DOTA-AgRP-6E in 400 μL of mouse serum at 37°C for 2 h. Afterward, the mixture was re-suspended in 0.5 mL of DMF containing 5 μL of Triton X-100 and centrifuged at 16,000 g for 2 min. The supernatant, which contained >95% of the starting radioactivity, was filtered using a 10 K NanoSep device (Pall Corporation, East Hills, NY, USA). Greater than 99% of the radioactive material passed through this filter. The samples were analyzed by radio-HPLC, and the percentage of intact peptide was determined by quantifying peaks corresponding to the intact peptide and to the degradation products.

2.5. In Vitro Cell Uptake Assay. Cell uptake studies were performed as previously described [16]. Briefly, U87MG cells were seeded at a density of 0.2 × 10^6 in 12-well tissue culture plates and allowed to attach overnight. After washing three times with serum-free DMEM, cells were incubated with ^{111}In-DOTA-AgRP-7C or ^{111}In-DOTA-AgRP-6E (0.5 μCi/well) with or without the integrin-binding peptidomimetic, c(RGDyK), (2 μg/well) at 37 or 4°C for 15, 60, and 120 min, respectively. Cells were washed three times with chilled PBS containing 0.2% BSA and dissolved

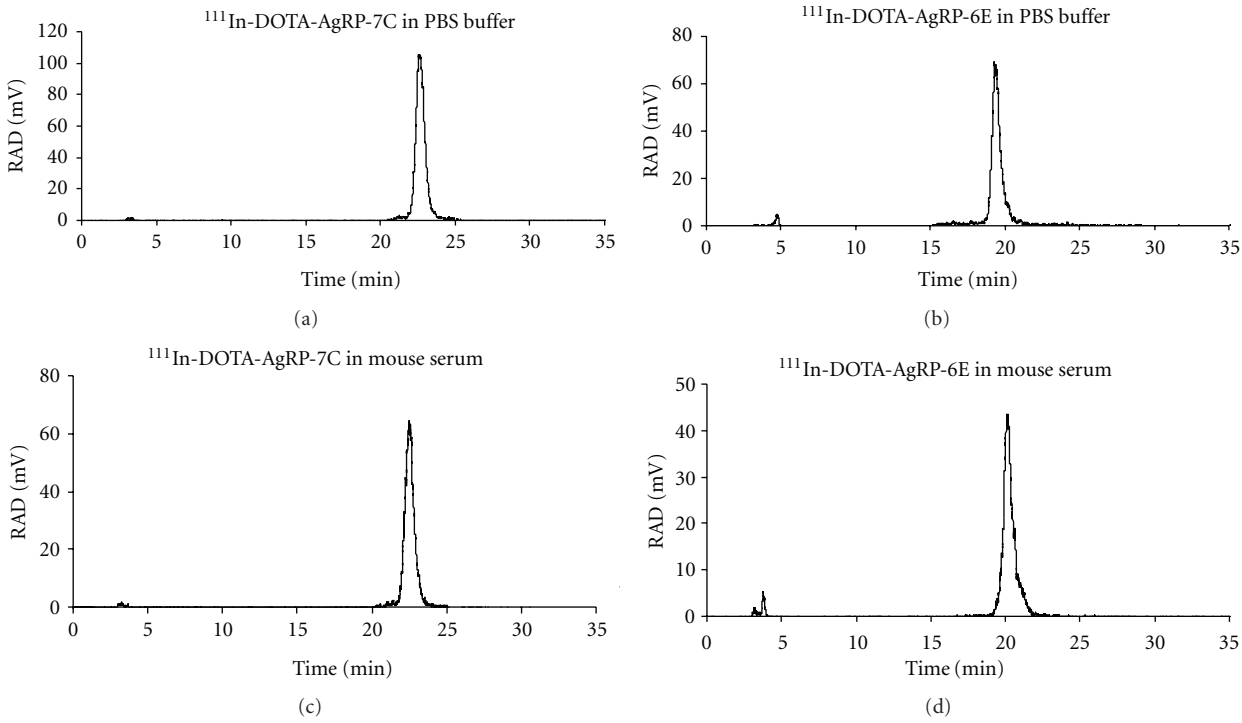

Figure 1: Stability analysis of ^{111}In-DOTA-AgRP-7C (a) and (b), and ^{111}In-DOTA-AgRP-6E (c) and (d) in PBS and mouse serum. The two radiopeptides were incubated with PBS for 24 h at room temperature, and mouse serum for 2 h at 37°C.

by treatment with 0.1 N NaOH at room temperature for 5 min. The cells' suspensions were collected and the resultant radioactivity was measured using a γ-counter (PerkinElmer 1470, Waltham, MA, USA). Cell uptake was expressed as the percentage of added radioactivity. Experiments were performed twice with triplicate wells.

2.6. Biodistribution Studies. All animal studies were carried out in compliance with federal and local institutional rules for animal experimentation. Approximately, 10^7 U87MG cells were suspended in PBS and subcutaneously implanted in the left shoulders of female athymic nu/nu mice. Tumors were allowed to grow to a size of 0.5 cm (2-3 weeks) before imaging experiments were performed. For biodistribution studies, U87MG tumor-bearing mice ($n = 3$ for each group) were injected with ^{111}In-DOTA-AgRP-7C (0.259–0.37 MBq, 7–10 Ci) or ^{111}In-DOTA-AgRP-6E (0.296–0.444 MBq, 8–12 μCi) via the tail vein and sacrificed at different time points (0.5, 2, 24, and 48 h) after injection (p.i.). Tumor and normal tissues of interest were removed and weighed, and their radioactivity was measured with a γ-counter. Radioactivity uptake was expressed as the percent injected dose per gram of tissue (%ID/g). To test the *in vivo* $\alpha_v\beta_3$ integrin targeting specificity of the probe, U87MG tumor-bearing mice ($n = 3$ for each group) were injected via the tail vein with a mixture of ^{111}In-DOTA-AgRP-7C (0.259–0.37 MBq, 7–10 μCi) and 330 μg of c(RGDyK). The mice were sacrificed at 2 h p.i. and the biodistribution of the radiolabeled peptide was measured as above.

2.7. Statistical Analysis. Quantitative data were expressed as mean ± SD. Means were compared using the Student *t*-test. A 95% confidence level was chosen to determine the significance between groups, with P values of less than 0.05 indicating significant differences.

3. Results

3.1. Radiolabeling. Due to the high thermal stability of cystine-knot peptides, DOTA-AgRP-6E and DOTA-AgRP-7C were easily labeled with $^{111}InCl_3$ by incubation in NH_4OAc buffer (pH 5.0–5.5) at 80°C for 45 min. Radiolabeled peptides were purified by PD-10 columns. The radiochemical yield for both peptides was determined by radio-HPLC to be ~50% and the radiochemical purity as also determined by radio-HPLC was greater than 99%. The specific activity of the peptides was determined to be approximately 0.25 mCi/nmol.

3.2. Peptide Stability. Both ^{111}In-DOTA-AgRP-7C and ^{111}In-DOTA-AgRP-6E were radiochemically stable after 24 h in 0.01 M PBS (pH 7.4), as determined by radio-HPLC analysis (Figures 1(a) and 1(c)). Furthermore, radio-HPLC analysis revealed that over 95% of the probes remained intact after 2 h incubation with mouse serum at 37°C (Figures 1(b) and 1(d)).

3.3. In Vitro Cell Uptake. The uptake of ^{111}In-DOTA-AgRP-7C and ^{111}In-DOTA-AgRP-6E was evaluated in U87MG

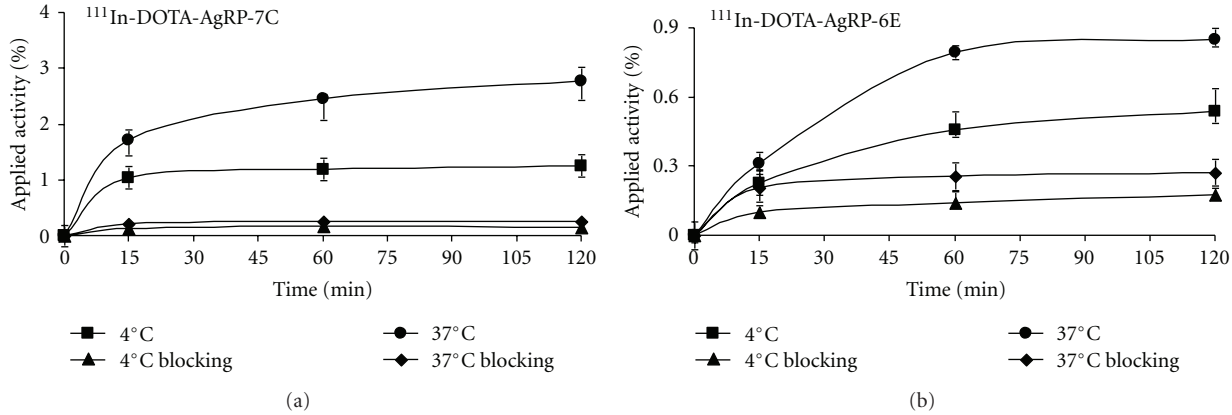

Figure 2: *In vitro* cell uptake assay of ^{111}In-DOTA-AgRP-7C (a) and ^{111}In-DOTA-AgRP-6E (b) on U87MG cells at 37°C and 4°C with or without c(RGDyK) blocking peptide ($n = 3$, mean ± SD).

cells and the results are shown in Figure 2. During the first 15 min incubation period at 37°C, ^{111}In-DOTA-AgRP-7C exhibited rapid cell accumulation, followed by a steady increase in binding and receptor-mediated uptake throughout the experiment. The cell uptake values of ^{111}In-DOTA-AgRP-7C after 15, 60 and 120 min at 37°C were 1.70 ± 0.07%, 2.46 ± 0.29%, and 2.76 ± 0.25%, and at 4°C were 1.05 ± 0.21%, 1.19 ± 0.27%, and 1.26 ± 0.38%, respectively (Figure 2(a)). Thus, a ~2 fold greater accumulation of probe was observed in cells incubated at 37°C compared to those incubated at 4°C, which is indicative of internalization that occurs at physiological temperature. Moreover, cell surface binding and internalization were significantly inhibited by the addition of a large molar excess of the integrin-binding peptidomimetic c(RGDyK) ($P < 0.05$) (Figure 2(a)). After 1 h, cell uptake of the probe was inhibited 90% and 86% at 37°C and 4°C, respectively, demonstrating that the probe specifically targets cell surface integrin receptors.

In comparison, the U87MG cell uptake values of ^{111}In-DOTA-AgRP-6E after 15, 60, and 120 min at 37°C were 0.32 ± 0.01%, 0.85 ± 0.28% and 0.96 ± 0.07%, and at 4°C were 0.22 ± 0.04%, 0.45 ± 0.04%, and 0.50 ± 0.05%, respectively (Figure 2(b)). Similar to ^{111}In-DOTA-AgRP-7C, a ~2-fold increase in uptake of ^{111}In-DOTA-AgRP-6E was found at 37°C compared to 4°C. Probe accumulation was blocked by the addition of c(RGDyK), with reductions in cell uptake of 38% at 37°C and 42% at 4°C after 1 h (Figure 2(b)).

3.4. Biodistribution Studies. The biodistribution of ^{111}In-DOTA-AgRP-7C was examined in nude mice bearing U87MG human glioblastoma tumors. The results of these experiments are shown in Table 2. Tumor uptake of the probe was 5.74 ± 1.60, 2.35 ± 0.36, 1.29 ± 0.02, and 0.76 ± 0.17%ID/g at 0.5, 2, 24, and 48 h, respectively, indicating relatively high tumor uptake and moderate tumor retention. The probe was found to have rapid blood clearance, with radioactivity levels of 0.68 ± 0.26 and 0.10 ± 0.02%ID/g remaining in the blood after 0.5 and 2 h p.i., respectively. Moreover, whole-body clearance of radioactivity was equally rapid. Except for the kidneys, accumulation in most organs examined were all lower than 1%ID/g at 2 h p.i. Prominent uptake was observed in the kidneys at early time points (33.93 ± 8.35%ID/g at 0.5 h), with decreasing accumulation from 2 to 48 h p.i. These data clearly indicate a renal excretion route and metabolic processing of the probe by the kidneys. With the rapid clearance of the radiotracer from blood and other normal organs, ^{111}In-DOTA-AgRP-7C exhibited high tumor-to-normal organ ratios in the blood, muscle, lung, liver, spleen, and pancreas (Table 2 and Figure 3(b)). For example, at 2 h p.i., the tumor-to-blood and tumor-to-muscle ratio of ^{111}In-DOTA-AgRP-7C was 25.8 and 39.8, respectively. To confirm *in vivo* integrin binding specificity, co-injection of ^{111}In-DOTA-AgRP-7C with a large molar excess of c(RGDyK) significantly reduced tumor uptake by ~77% (0.54 ± 0.07 versus 2.35 ± 0.36%ID/g at 2 h p.i., $P < 0.05$) (Table 2). Significant differences were also found for probe uptake in normal tissues such as spleen upon addition of c(RGDyK) blocking peptide.

The biodistribution results of ^{111}In-DOTA-AgRP-6E are summarized in Table 3. Intermediate tumor uptake of ^{111}In-DOTA-AgRP-6E was observed at 0.5, 2, and 24 h p.i., with values of 1.76 ± 0.34, 1.21 ± 0.21, and 0.89 ± 0.06%ID/g, respectively. The probe also showed rapid blood clearance, with radioactivity levels of 1.27 ± 0.53 and 0.06 ± 0.05%ID/g remaining in the blood after 0.5 and 2 h. In addition, low normal tissue accumulation was seen with the exception of the kidneys (15.37 ± 3.19%ID/g and 14.68 ± 1.98%ID/g at 0.5 and 2 h, resp.). Finally, because of the rapid clearance of the probe from the blood and other organs, ^{111}In-DOTA-AgRP-6E also displayed high tumor-to-blood and tumor-to-muscle ratios at 2 and 24 h p.i. (Table 3).

4. Discussion

The native AgRP is a neuropeptide produced in the human brain that plays an important biological role in increasing appetite and decreasing metabolism and energy expenditure [17–19]. The C-terminus of AgRP is a cystine-knot peptide which contains a biologically active loop that naturally binds to melanocortin receptors. A truncated form of the AgRP

Table 2: Biodistribution results for ^{111}In-DOTA-AgRP-7C in nude mice bearing subcutaneous U87MG human glioblastoma xenografts. Data are expressed as the percent injected dose per gram of tissue (%ID/g) after intravenous injection of the probe (0.259–0.37 MBq, 7–10 μCi) at 0.5, 2, 24, and 48 h ($n = 3$). For 2 h blocking group, mice were coinjected with 330 μg of c(RGDyK).

Tissues	0.5 h	2 h	24 h	48 h	2 h Blocking
%ID/g					
Tumor	5.74 ± 1.60	2.35 ± 0.36	1.29 ± 0.02	0.76 ± 0.17	0.54 ± 0.07*
Brain	0.04 ± 0.02	0.02 ± 0.01	0.01 ± 0.00	0.01 ± 0.01	0.01 ± 0.00
Blood	0.68 ± 0.26	0.10 ± 0.02	0.01 ± 0.00	0.01 ± 0.00	0.07 ± 0.01
Heart	0.45 ± 0.16	0.12 ± 0.02	0.04 ± 0.01	0.03 ± 0.00	0.06 ± 0.01
Lung	2.11 ± 0.65	0.86 ± 0.20	0.26 ± 0.09	0.12 ± 0.02	0.41 ± 0.08
Liver	0.80 ± 0.19	0.43 ± 0.16	0.24 ± 0.03	0.19 ± 0.03	0.20 ± 0.04
Spleen	1.70 ± 0.62	0.88 ± 0.21	0.58 ± 0.09	0.46 ± 0.10	0.21 ± 0.03*
Kidneys	33.93 ± 8.35	30.59 ± 4.62	19.12 ± 2.17	8.47 ± 0.04	34.52 ± 4.02
Muscle	0.30 ± 0.13	0.06 ± 0.01	0.04 ± 0.01	0.02 ± 0.01	0.10 ± 0.10
Pancreas	0.42 ± 0.17	0.13 ± 0.03	0.09 ± 0.01	0.05 ± 0.01	0.13 ± 0.03
Bone	1.41 ± 0.36	0.63 ± 0.05	0.39 ± 0.07	0.24 ± 0.05	0.45 ± 0.01
Stomach	2.17 ± 0.49	0.80 ± 0.06	0.21 ± 0.01	0.14 ± 0.02	0.24 ± 0.04*
Intestine	2.02 ± 0.71	0.60 ± 0.13	0.29 ± 0.02	0.22 ± 0.03	0.25 ± 0.06*
Ratio					
Tumor-to-blood	8.90 ± 3.09	25.81 ± 10.46	127.53±30.50	144.12±36.33	8.18 ± 0.15*
Tumor-to-muscle	20.56 ± 6.40	39.83 ± 9.16	37.69 ± 9.81	41.12 ± 8.62	14.03±13.45*

*$P < 0.05$ compared with ^{111}In-DOTA-AgRP-7C without c(RGDyK) blocking at 2 h. Data are presented as mean ± SD ($n = 3$).

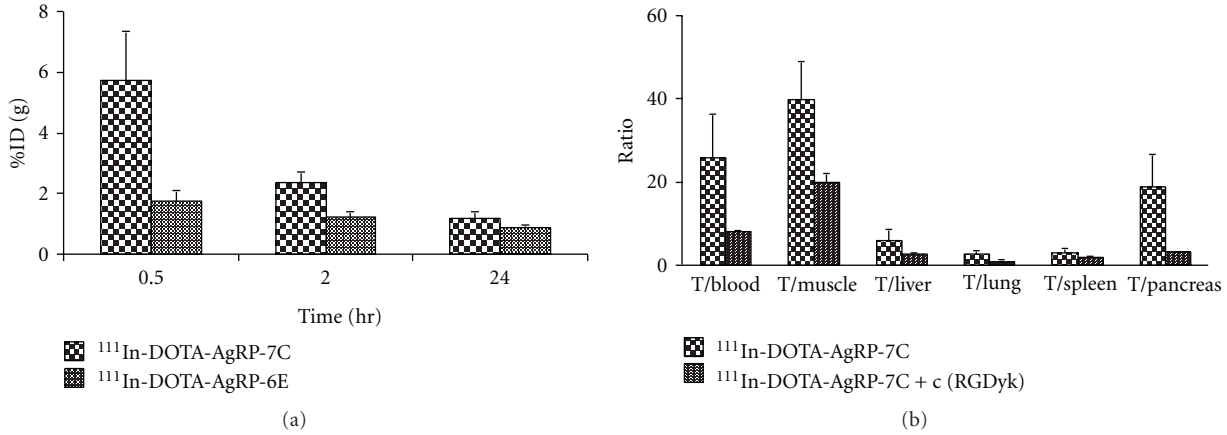

Figure 3: U87MG tumor uptake for ^{111}In-DOTA-AgRP-7C and ^{111}In-DOTA-AgRP-6E at 0.5, 2, and 24 h p.i. (a). Tumor (T)-to-normal organ ratios for ^{111}In-DOTA-AgRP-7C with or without c(RGDyK) blocking peptide at 2 h after the injection of the probe (b).

cystine knot peptide, AgRP* is emerging as a highly attractive platform for developing novel molecular imaging probes [20, 21]. AgRP* is small in size (~4 kDa) and possesses a rigid structure, yet contains four solvent-accessible loops that could be used for mutagenesis [8]. In addition, peptides based on AgRP* are likely to be nonimmunogenic due to their human origin and high thermal and proteolytic stability; Furthermore, AgRP* is amenable to recombinant and synthetic production, which will allow site-specific incorporation of labels or chemical functionality in future studies.

In our previous studies, the AgRP*-based $\alpha_v\beta_3$ integrin binder AgRP-7C was discovered and used for PET imaging of tumor angiogenesis [8, 13]. Excellent *in vivo* tumor imaging contrast was achieved which demonstrates the success of using AgRP*-based scaffolds for molecular probe development [13]. This study motivated us to further evaluate engineered AgRP*-based integrin targeting peptides for potential SPECT imaging applications. The high affinity binder DOTA-AgRP-7C (IC_{50} ~20 nM) and moderate affinity binder DOTA-AgRP-6E (IC_{50} ~130 nM) were radiolabeled with ^{111}In and tested for their ability to target tumors in living subjects.

The cystine-knot motif of AgRP* conferred high stability to the radiolabeled peptides. Compared to the reaction temperature (37°C) used for ^{64}Cu radiolabeling of AgRP-7C,

Table 3: Biodistribution results for ^{111}In-DOTA-AgRP-6E in nude mice bearing subcutaneous U87MG human glioblastoma xenografts. Data are expressed as the percent %ID/g after intravenous injection of the probe (0.296–0.444 MBq, 8–12 μCi) at 0.5, 2, and 24 h ($n = 3$).

Tissue	0.5 h	2 h	24 h
%ID/g			
Tumor	1.76 ± 0.34	1.21 ± 0.21	0.89 ± 0.06
Brain	0.06 ± 0.01	0.02 ± 0.01	0.02 ± 0.01
Blood	1.27 ± 0.53	0.06 ± 0.05	0.01 ± 0.00
Heart	0.80 ± 0.24	0.18 ± 0.06	0.12 ± 0.02
Lung	1.86 ± 0.56	0.54 ± 0.12	0.27 ± 0.02
Liver	0.87 ± 0.20	0.52 ± 0.01	0.48 ± 0.02
Spleen	1.36 ± 0.26	0.83 ± 0.05	0.65 ± 0.06
Kidneys	15.37 ± 3.19	14.68 ± 1.98	6.87 ± 1.19
Muscle	0.64 ± 0.09	0.15 ± 0.07	0.07 ± 0.01
Pancreas	0.57 ± 0.23	0.20 ± 0.06	0.14 ± 0.01
Bone	1.18 ± 0.15	0.56 ± 0.10	0.36 ± 0.04
Stomach	2.02 ± 0.47	0.87 ± 0.14	0.53 ± 0.02
Intestine	2.04 ± 0.54	1.13 ± 0.14	0.93 ± 0.04
Ratio			
Tumor-to-blood	1.71 ± 1.21	33.04 ± 23.28	142.32 ± 3.39
Tumor-to-muscle	2.75 ± 0.28	9.20 ± 3.88	13.07 ± 1.94

Data are presented as mean ± SD ($n = 3$).

^{111}In radiolabeling of DOTA-AgRP-7C and DOTA-AgRP-6E was performed at 80°C. The high reaction temperature did not appear to denature the peptides as demonstrated by the cell uptake and biodistribution studies. Similar to ^{64}Cu-DOTA-AgRP-7C, both ^{111}In-DOTA-AgRP-7C and ^{111}In-DOTA-AgRP-6E were found to be stable in PBS buffer for at least 24 h and in mouse serum for 2 h.

In biodistribution studies, ^{111}In-DOTA-AgRP-7C shows rapid tumor targeting and uptake in integrin $\alpha_v\beta_3$ expressing human glioblastoma xenografts (5.74 ± 1.60%ID/g at 0.5 h), which is significant higher than that of ^{64}Cu-DOTA-AgRP-7C (1.92 ± 0.48%ID/g at 0.5 h, $P < 0.05$). Moreover, ^{111}In-DOTA-AgRP-7C shows fast blood clearance (0.68 ± 0.26%ID/g at 0.5 h), through the kidney-urinary system. The kidney uptake of ^{111}In-DOTA-AgRP-7C is 30.59 ± 4.62%ID/g at 2 h p.i., which is much lower than that of ^{64}Cu-DOTA-AgRP-7C (60.22 ± 17.52%ID/g at 2 h). Lastly, the uptake and retention of ^{111}In-DOTA-AgRP-7C in other normal organs is low (Table 2). Overall, these data indicate that using a different radiometal (^{111}In compared to ^{64}Cu) preserves the tumor targeting ability of engineered cystine-knot peptides, but significantly improves the *in vivo* performance of the resulting probe.

Both ^{111}In and ^{64}Cu labeled DOTA-AgRP-7C exhibit high renal uptake, which is likely attributed to (1) the long residence time of radiometabolites produced by lysosomal degradation of the radiolabeled peptides within renal cells; (2) the overall positive charge of the peptides [22–25]. Several strategies previously reported that the accumulation of radiopeptide in the kidneys can be effectively reduced by coinjection of cationic amino acid such as lysine, or polylysine molecules [16, 26]. These methods could potentially be explored to reduce the radiation dose to kidney.

Biodistribution studies reveal that ^{111}In-DOTA-AgRP-7C has significant higher tumor uptake than that of ^{111}In-DOTA-AgRP-6E at different time points (0.5, 2, and 24 h) (Figure 3(a)). This could be related to the stronger integrin binding affinity of AgRP-DOTA-7C compared to AgRP-DOTA-6E (IC_{50}: 22.6 ± 3.9 nM versus 125.5 ± 16.6 nM, resp.) [27]. Both probes display good retention in tumor and low uptakes in most of normal organs (Tables 2 and 3). Interestingly, the kidney uptake of ^{111}In-DOTA-AgRP-6E was significantly lower than that of ^{111}In-DOTA-AgRP-7C (14.68 versus 30.59%ID/g at 2 h p.i.), suggesting that modification of the amino acid sequence of the engineered loop of AgRP* may help to optimize *in vivo* behavior. Because ^{111}In-DOTA-AgRP-7C showed higher tumor uptake compared to ^{111}In-DOTA-AgRP-6E, the *in vivo* integrin targeting specificity of the probe was further confirmed by a blocking study, using a peptidomimetic (c(RGDyK)) that binds to the same epitope on integrin receptors. Compared to the nonblocking group, the tumor uptake of ^{111}In-DOTA-AgRP-7C is significantly decreased upon co-injection of c(RGDyK) (2.35 ± 0.36 versus 0.54 ± 0.07%ID/g at 2 h, resp.) Table 2 and Figure 3(b), in agreement with the *in vitro* cell uptake results.

In a previous study, the tumor uptake of ^{111}In-DOTA-c(RGDfK) was reported as 6.28%ID/g at 1 h p.i. in a SKOV3 xenograft model [28]. In comparison, we show that the tumor uptake of ^{111}In-DOTA-AgRP-7C is 5.74%ID/g at 0.5 h p.i. in a U87MG xenograft model. Importantly, ^{111}In-DOTA-AgRP-7C and ^{111}In-DOTA-AgRP-6E were found to have much lower uptake and faster clearance in liver, lung, spleen and other normal tissues compared to ^{111}In-DOTA-c(RGDfK). The fast clearance of ^{111}In-labeled AgRP* mutants resulted in high tumor-to-blood and tumor-to-muscle ratios at 24 and 48 h p.i. (Tables 2 and 3,

Figure 3), demonstrating the advantages of using an AgRP*-based scaffold for imaging probe development [28, 29].

5. Conclusions

In summary, we tested the $\alpha_v\beta_3$ integrin-targeted cystine-knot peptides ^{111}In-DOTA-AgRP-6E and ^{111}In-DOTA-AgRP-7C as SPECT imaging agents in mouse tumor models. Compared to ^{111}In-DOTA-AgRP-6E, ^{111}In-DOTA-AgRP-7C exhibits higher integrin binding affinity and tumor uptake. Moreover, this probe demonstrates rapid tumor uptake, high tumor-to-normal tissue contrast, and favorable pharmacokinetics. These results suggest that AgRP* mutant 7C has potential for clinical translation as a new SPECT imaging agent for integrin $\alpha_v\beta_3$ positive tumors. Furthermore, cystine-knot peptides are a promising class of molecular scaffolds, and warrant further development and investigation for imaging applications.

Conflict of Interests

The authors declare that they have no conflict of interests.

Acknowledgments

This work was supported, in part, by National Cancer Institute (NCI) NCI 5 R01 CA119053 (to Z. Cheng), NCI *In Vivo* Cellular Molecular Imaging Center (ICMIC) Grant P50 CA114747, NCI 5K01 CA104706 (to J. R. Cochran), and a Stanford Molecular Imaging Scholars postdoctoral fellowship R25 CA118681 (to R. H. Kimura). Moreover, this work was also funded by the National Science Foundation for Young Scholars of China (Grant no. 81101072) and Shanghai Health Bureau Research Funding for Young Scholars (Grant no. 20114Y161) (to L. Jiang).

References

[1] T. Saga, M. Koizumi, T. Furukawa, K. Yoshikawa, and Y. Fujibayashi, "Molecular imaging of cancer—evaluating characters of individual cancer by PET/SPECT imaging," *Cancer Science*, vol. 100, no. 3, pp. 375–381, 2009.

[2] R. Weissleder and U. Mahmood, "Molecular imaging," *Radiology*, vol. 219, no. 2, pp. 316–333, 2001.

[3] T. F. Massoud and S. S. Gambhir, "Molecular imaging in living subjects: seeing fundamental biological processes in a new light," *Genes and Development*, vol. 17, no. 5, pp. 545–580, 2003.

[4] S. Mather, "Molecular imaging with bioconjugates in mouse models of cancer," *Bioconjugate Chemistry*, vol. 20, no. 4, pp. 631–643, 2009.

[5] W. A. Weber, "Positron emission tomography as an imaging biomarker," *Journal of Clinical Oncology*, vol. 24, no. 20, pp. 3282–3292, 2006.

[6] H. Kolmar, "Biological diversity and therapeutic potential of natural and engineered cystine knot miniproteins," *Current Opinion in Pharmacology*, vol. 9, no. 5, pp. 608–614, 2009.

[7] H. Kolmar, "Alternative binding proteins: biological activity and therapeutic potential of cystine-knot miniproteins," *FEBS Journal*, vol. 275, no. 11, pp. 2684–2690, 2008.

[8] A. P. Silverman, A. M. Levin, J. L. Lahti, and J. R. Cochran, "Engineered cystine-knot peptides that bind $\alpha_v\beta_3$ integrin with antibody-like affinities," *Journal of Molecular Biology*, vol. 385, no. 4, pp. 1064–1075, 2009.

[9] R. O. Hynes, "Integrins: versatility, modulation, and signaling in cell adhesion," *Cell*, vol. 69, no. 1, pp. 11–25, 1992.

[10] R. E. B. Seftor, E. A. Seftor, K. R. Gehlsen et al., "Role of the $\alpha_v\beta_3$ integrin in human melanoma cell invasion," *Proceedings of the National Academy of Sciences of the United States of America*, vol. 89, no. 5, pp. 1557–1561, 1992.

[11] P. C. Brooks, R. A. F. Clark, and D. A. Cheresh, "Requirement of vascular integrin $\alpha_v\beta_3$ for angiogenesis," *Science*, vol. 264, no. 5158, pp. 569–571, 1994.

[12] E. Chang, S. Liu, G. Gowrishankar et al., "Reproducibility study of [^{18}F]FPP(RGD)$_2$ uptake in murine models of human tumor xenografts," *European Journal of Nuclear Medicine and Molecular Imaging*, vol. 38, no. 4, pp. 722–730, 2011.

[13] L. Jiang, R. H. Kimura, Z. Miao et al., "Evaluation of a ^{64}Cu-labeled cystine-knot peptide based on agouti-related protein for PET of tumors expressing $\alpha_v\beta_3$ integrin," *Journal of Nuclear Medicine*, vol. 51, no. 2, pp. 251–258, 2010.

[14] J. Yang, H. Guo, and Y. Miao, "Technetium-99m-labeled Arg-Gly-Asp-conjugated alpha-melanocyte stimulating hormone hybrid peptides for human melanoma imaging," *Nuclear Medicine and Biology*, vol. 37, no. 8, pp. 873–883, 2010.

[15] Z. Xiong, Z. Cheng, X. Zhang et al., "Imaging chemically modified adenovirus for targeting tumors expressing integrin $\alpha_v\beta_3$ in living mice with mutant herpes simplex virus type 1 thymidine kinase PET reporter gene," *Journal of Nuclear Medicine*, vol. 47, no. 1, pp. 130–139, 2006.

[16] Z. Cheng, J. Chen, T. P. Quinn, and S. S. Jurisson, "Radioiodination of rhenium cyclized α-melanocyte-stimulating hormone resulting in enhanced radioactivity localization and retention in melanoma," *Cancer Research*, vol. 64, no. 4, pp. 1411–1418, 2004.

[17] M. Bäckberg, N. Madjid, S. O. Ögren, and B. Meister, "Down-regulated expression of agouti-related protein (AGRP) mRNA in the hypothalamic arcuate nucleus of hyperphagic and obese tub/tub mice," *Molecular Brain Research*, vol. 125, no. 1-2, pp. 129–139, 2004.

[18] J. R. Shutter, M. Graham, A. C. Kinsey, S. Scully, R. Lüthy, and K. L. Stark, "Hypothalamic expression of ART, a novel gene related to agouti, is up-regulated in obese and diabetic mutant mice," *Genes and Development*, vol. 11, no. 5, pp. 593–602, 1997.

[19] M. M. Ollmann, B. D. Wilson, Y. K. Yang et al., "Antagonism of Central Melanocortin receptors in vitro and in vivo by agouti-related protein," *Science*, vol. 278, no. 5335, pp. 135–138, 1997.

[20] P. J. Jackson, J. C. McNulty, Y. K. Yang et al., "Design, pharmacology, and NMR structure of a minimized cystine knot with agouti-related protein activity," *Biochemistry*, vol. 41, no. 24, pp. 7565–7572, 2002.

[21] P. J. Jackson, N. R. Douglas, B. Chai et al., "Structural and molecular evolutionary analysis of Agouti and Agouti-related proteins," *Chemistry and Biology*, vol. 13, no. 12, pp. 1297–1305, 2006.

[22] S. R. Kumar and S. L. Deutscher, "^{111}In-labeled galectin-3-targeting peptide as a SPECT agent for imaging breast tumors," *Journal of Nuclear Medicine*, vol. 49, no. 5, pp. 796–803, 2008.

[23] C. E. Mogensen and K. Solling, "Studies on renal tubular protein reabsorption: partial and near complete inhibition by certain amino acids," *Scandinavian Journal of Clinical and Laboratory Investigation*, vol. 37, no. 6, pp. 477–486, 1977.

[24] S. Silbernagl, "The renal handling of amino acids and oligopeptides," *Physiological Reviews*, vol. 68, no. 3, pp. 911–1007, 1988.

[25] J. Q. Chen, Z. Cheng, N. K. Owen et al., "Evaluation of an 111In-DOTA-rhenium cyclized α-MSH analog: a novel cyclic-peptide analog with improved tumor-targeting properties," *Journal of Nuclear Medicine*, vol. 42, no. 12, pp. 1847–1855, 2001.

[26] J. Q. Chen, Z. Cheng, T. J. Hoffman, S. S. Jurisson, and T. P. Quinn, "Melanoma-targeting properties of ^{99m}technetium-labeled cyclic α-melanocyte-stimulating hormone peptide analogues," *Cancer Research*, vol. 60, no. 20, pp. 5649–5658, 2000.

[27] L. Jiang, Z. Miao, R. H. Kimura et al., "Preliminary evaluation of ^{177}Lu-labeled knottin peptides for integrin receptor-targeted radionuclide therapy," *European Journal of Nuclear Medicine and Molecular Imaging*, vol. 38, no. 4, pp. 613–622, 2011.

[28] M. Yoshimoto, K. Ogawa, K. Washiyama et al., "$\alpha_v\beta_3$ integrin-targeting radionuclide therapy and imaging with monomeric RGD peptide," *International Journal of Cancer*, vol. 123, no. 3, pp. 709–715, 2008.

[29] M. L. Janssen, W. J. Oyen, I. Dijkgraaf et al., "Tumor targeting with radiolabeled $\alpha_v\beta_3$ integrin binding peptides in a nude mouse model," *Cancer Research*, vol. 62, no. 21, pp. 6146–6151, 2002.